On-demand semiconductor source of entangled photons with high efficiency and indistinguishability

Hui Wang, Hai Hu, T. H. Chung, Qin Jian, Xiaoxia Yang, Jin-Peng Li, Ren-Ze Liu, Han-Sen Zhong, Yu-Ming He, Xing Ding, Yu-Hao Deng, C. Schneider, Qing Dai, Yong-Heng Huo, Sven Höfling, Chao-Yang Lu and Jian-Wei Pan

[1] *Hefei National Laboratory for Physical Sciences at Microscale and Department of Modern Physics, University of Science and Technology of China, Hefei, Anhui, 230026, China*
[2] *CAS Centre for Excellence and Synergetic Innovation Centre in Quantum Information and Quantum Physics, University of Science and Technology of China, Hefei, Anhui 230026, China*
[3] *Nanophotonics Research Division, CAS Center for Excellence in Nanoscience, National Center for Nanoscience and Technology, Beijing, 100190, China*
[4] *Technische Physik, Physikalisches Instität and Wilhelm Conrad Röntgen-Center for Complex Material Systems, Universitat Würzburg, Am Hubland, D-97074 Würzburg, Germany*
[5] *SUPA, School of Physics and Astronomy, University of St. Andrews, St. Andrews, KY16 9SS, United Kingdom*

Abstract:

An outstanding goal in quantum optics and scalable photonic quantum technology is to develop a source that each time emits one and only one entangled photon pair with simultaneously high entanglement fidelity, extraction efficiency, and photon indistinguishability. By coherent two-photon excitation of a single InGaAs quantum dot coupled to a circular Bragg grating bullseye cavity with broadband Purcell enhancement, we generate entangled photon pairs with a state fidelity of 0.90(1), single-photon extraction efficiency of 0.79(1), and photon indistinguishability up to 0.93(1) simultaneously. Our work will open up many applications in high-efficiency multi-photon experiments and solid-state quantum repeaters.

Quantum entanglement [1] between flying photons [2] are central in the Bell test [3] of the contradiction between local hidden variable theory and quantum mechanics [4]. Aside from the fundamental interest, the entangled photons have been recognized as the elementary resources in quantum key distribution [5], quantum teleportation [6], quantum metrology [7] and quantum computing [8]. There has been a strong interest in experimental generations of entangled photons from trapped atoms [9], spontaneous parametric down-conversion (SPDC) [10], and quantum dots [11] etc. A checklist of relevant parameters for an entangled-photon pair source include [12]:

A. Entanglement fidelity. The produced two photons should be in a state close to a maximally entangled Bell state;

B. On-demand generation. The source should, at a certain time, emit one and only one pair of entangled photons;

C. Collection efficiency. The photons should be extracted out from the source and collected with a high efficiency;

D. Indistinguishability. The photons emitted from different trials should be exactly identical in all degrees of freedom.

The past decades witnessed increasingly more sophisticated Bell tests and advanced photonic quantum information technologies enabled by developments of the photon entanglement source striving to fulfill the four criteria. For example, by combining **A** and **C**, the SPDC photons allowed for Bell tests closing both the locality and detection loopholes simultaneously [13, 14]. Very recently, ultrafast pulsed SPDC satisfied **A**, **C**, and **D** and was exploited to demonstrate 12-photon entanglement and scattershot boson sampling [15]. However, the item **B** remains an intrinsic problem for the SPDC where the photon pairs are generated probabilistically, and inevitably accompanied with undesirable multi-pair emissions.

An alternative route to generate entangled photons is through radiative cascades in single quantum emitters such as quantum dots which can have a near-unity quantum efficiency [11], therefore meeting the item **B**. However, the solid-state artificial atom system has its own challenges, including the structural symmetry, extraction efficiency,

and dephasings. To this end, tremendous progress has been reported in eliminating the fine structure splitting of neutral excitons [16-18], improving the extraction efficiency using double-micropillar structures [19] or broadband antennas [20-22], and enhancing the entanglement fidelity and photon indistinguishability using resonant excitation [23, 24]. Encouragingly, the entanglement fidelity (**A**) and the photon indistinguishability (**D**) (for 2 ns separation) has reached 0.978(5) and 0.93(7), respectively [18, 24]. Very recently, the entanglement fidelity of 0.9 (**A**) was combined with a record-high pair extraction efficiency of 0.37 per pulse (**C**) on the same device [22].

Despite these progress, it remained an outstanding challenge to simultaneously fulfill all the criteria **A**-**D**, which is crucial for the photon entanglement source to be useful for many applications such as quantum repeaters [25] and optical quantum computing [26]. For example, efficiently “fusing” entangled photon pairs into large-scale cluster states relies on high entanglement fidelity, quantum interference visibility and heralding efficiency all together [27].

In this Letter, we report a near-perfect entangled-photon source that for the first time fulfills **A**-**D**. By coherently driving a single InGaAs quantum dot coupled to a bullseye microcavity with broadband Purcell enhancement, we create entangled photons with a fidelity of 0.90(1), extraction efficiency of 0.79(1), and photon indistinguishability up to 0.93(1) simultaneously.

While polarized single-photon sources from quantum dot-micropillars with both high efficiency and photon indistinguishability have been demonstrated very recently [28], the creation of near-perfect entangled photon pairs posed additional challenges. First, the fine structure splitting should be smaller than the radiative linewidth of the single photons, leaving no room for leaking which-path information. Second, as the two single photons from the biexciton-exciton (XX-X) radiative cascaded emission have different wavelengths, broadband Purcell-cavities should be used to enhance both the XX and X photons. The Purcell factor that can accelerate the radiative decay rate, together with resonant excitation without inducing dephasing and emission time jitter, is desirable both for improving the two-photon entanglement fidelity and indistinguishability.

We choose self-assembled InGaAs quantum dots as single quantum emitters which can have near-unity quantum efficiencies [29]—a prerequisite for the criteria **B**—and near-transform-limited emission linewidth [30]. For a broadband high-Purcell cavity, we adopt circular Bragg grating (CBG) in a bullseye geometry [31] which features a small effective mode volume and a relatively low Q factor (~150). The CBGs have been previously employed to enhance the single-photon collection from quantum dots [32] and nitrogen vacancy centers in diamond [33]. A scanning electron microscope image of our CBG device is shown in Fig. 1a. We design the parameters of the CBG as detailed in Fig. 1b in order to align its resonance with a moderate spectral range of ~5 nm to the center of the wavelength of the photon pairs (see the caption of Fig. 1 and supplemental materials for more details).

To redirect the single photon emission from downward back to upward, a gold mirror is fabricated at the bottom of the quantum dot. The idea of backside metallic broadband mirror has been used in quantum dots membranes and embedded in nanowire [34], solid immersion lens and antennas [22, 35], etc. A 360 nm thick SiO_2 is sandwiched between the GaAs membrane and the gold mirror, forming a constructive interference between the downward and upward light. Our numerical simulation in Fig. 1c shows that for our chosen parameters, a Purcell factor of ~20 and an extraction efficiency (defined as the ratio of single photons escaped from bulk GaAs and collected into the first lens) up to 90% can be achieved for both the X and XX photons. Another key issue to check is that whether the emitted photons can be efficiently collected into a single-mode fiber. We simulate the far field intensity distribution using finite-different time-domain method. The numerical results (see in Fig. 1d) shows that the single-photon emission is highly directional and slightly elliptical. An objective lens with a numerical aperture (NA) of 0.65 is capable of collecting ~90% of the emitted photons.

As illustrated in the inset of Fig. 2a, our scheme to generate entangled photons is via XX-X cascade radiative decay in an InGaAs quantum dot. The polarization of emitted photons is determined by the spin of the intermediate exciton states. In our sample, ~ 3% of the quantum dots show fine structure splitting below 2.5 μeV. We pick a quantum

dot with a small fine structure splitting of <1.2 μeV, which is limited by the resolution of the spectrometer. We use coherent two-photon excitation scheme [23] to pump the quantum dot to the XX state. The energy of the pump pulsed laser is set at the average energy of the XX and X photons. We observe a clean photon pair emission spectrum as shown in Fig. 2a, where the X and XX lines are separated by ~1.6 nm.

We vary the average power of the laser and record the photon counts with a nanowire superconducting single-photon detector. The data for both XX and X photons are shown in Fig. 2b, where we observe clear Rabi oscillations due to a coherent control of the quantum dot biexcitonic system [23]. The XX and X photon count rates reach their first maxima at π pulses under a pumping laser power of ~16 nW. Such a power is ~ 3 orders of magnitudes lower than in non-resonant excitations where the photon counts usually grow asymptotically with pump power [16, 19]. The efficient excitation requiring only very low pump power is important for eliminating the undesired multiexciton states and fluctuating electrical noise in the vicinity of the quantum dot.

Under a pumping rate of 76 MHz and at π pulse, the final count rates observed in our experimental set-up are $4.41\times10^{6}/s$ and $4.34\times10^{6}/s$ for the XX and X photons, respectively. By bookkeeping independently calibrated single-photon detection efficiency (~76%), optical path transmission rate (~25%, including optical window, grating, two beam splitters and fiber connectors), and single-mode fiber coupling efficiency (~65%), XX excited-state preparation efficiency at π pulse and radiation efficiency (~70%), blinking (~84%), we estimate that 79.5% (78.2%) of the generated XX (X) single photons are collected into the first objective lens (NA=0.68). Thus the photon pair extraction efficiency is 62.2% (criteria **C**).

The record high photon counts observed in Fig. 2b suggest a strong Purcell coupling with single quantum emitters. To quantify the Purcell factor, we perform time-resolved resonance fluorescence measurements under the two-photon excitation to extract the radiative lifetimes of the XX and X photons (Fig. 2c), which are 66.4(1) ps and 126.7(4) ps, respectively, shortened by a factor of 11.3 and 8.7 compared to the quantum dot in bulk GaAs. The Purcell factor of the XX photon is higher than that of the X photon,

which is due to a better spectral match to the cavity (see supplemental materials). The CBG cavity not only gives comparable Purcell factors as those in the state-of-the-art micropillar-quantum dot single-photon devices [28], more interestingly, it also works over a moderately broadband over a few nanometers.

The XX and X photons are first characterized separately by second-order correlation measurements. Owing to the two-photon excitation scheme that spectrally separates the scattering laser from the emitted photons, near background-free entangled photons can be obtained [36]. This is confirmed by the accumulated intensity-correlation histogram in Fig. 2d, where at π pulse, nearly vanishing double-photon emission probabilities, $g^2_{\mathrm{XX}}(0) = 0.014(1)$, and $g^2_{\mathrm{X}}(0) = 0.013(1)$, are observed at zero time delay without any background subtraction. The strong anti-bunching reveals a near-perfect single-photon nature even under saturation pumping, without any fundamental tradeoff between the generation efficiency and the single-photon purity (criterion **B**), an intrinsic advantage compared to the parametric down-conversion [10] where increasing the photon pair rate inevitably induces more higher-order photon emission.

Next, we characterize the entangled photons by measuring their state fidelity, that is, the overlap of our experimentally produced states with an ideal, maximally entangled state (criterion **A**). We perform polarization-resolved cross-correlation measurements between the XX and X photons. The correlations at three mutually unbiased basis, right (R) and left (L) circular, horizontal (H) and vertical (V), diagonal (D) and anti-diagonal (A), are plotted in Fig. 3. In the linear and diagonal basis (see Fig. 3a and 3b), the measured histograms show a strong bunching when XX and X photons have parallel polarizations and an antibunching when they are orthogonal. The data in the circular basis (see Fig. 3c) shows an opposite behavior. The data suggests that the entangled two-photon state is close to the form of $|\psi\rangle_{XX,X} = (|H\rangle_{XX}|H\rangle_X + |V\rangle_{XX}|V\rangle_X)/\sqrt{2}$. The correlation visibilities for each basis should be calculated by:

$$V_{\mathrm{basis}} = \frac{g^2_{\mathrm{XX,X}}(0) - g^2_{\mathrm{XX,\overline{X}}}(0) - g^2_{\mathrm{\overline{XX},X}}(0) + g^2_{\mathrm{\overline{XX},\overline{X}}}(0)}{g^2_{\mathrm{XX,X}}(0) + g^2_{\mathrm{XX,\overline{X}}}(0) + g^2_{\mathrm{\overline{XX},X}}(0) + g^2_{\mathrm{\overline{XX},\overline{X}}}(0)},$$

where $g^2_{\mathrm{XX,X}}(0)$, $g^2_{\mathrm{XX},\overline{\mathrm{X}}}(0)$ are the coincidences of co-polarized bases, and $g^2_{\mathrm{XX},\overline{\mathrm{X}}}(0)$, $g^2_{\overline{\mathrm{XX}},\mathrm{X}}(0)$ are those of cross-polarized bases. From a complete and necessary set of 12 measurements as plotted in Fig. 3, we extract $V_{\mathrm{linear}} = 0.84(1)$, $V_{\mathrm{diagonal}} = 0.86(1)$, and $V_{\mathrm{circular}} = -0.88(1)$. Thus, the fidelity to the maximally entangled state is obtained as $F = (1 + V_{\mathrm{linear}} + V_{\mathrm{diagonal}} - V_{\mathrm{circular}})/4 = 0.90(1)$. We note that here the high Purcell factor broadens the intrinsic linewidth of the photons and thus a larger fine structure splitting can be tolerated, which is favorable for a high-fidelity two-photon entanglement. The residual fine structure splitting can be further eliminated to nearly zero by strain tuning [18], a technique perfectly compatible with the current membrane structure.

Having simultaneously fulfilled the criteria **A**, **B**, and **C**, finally we turn to test the **D**: photon indistinguishability. The quantum dot is excited every 13.1 ns by two π pulses separated by 1 ns. Hong-Ou-Mandel interference between the two consecutive photons is performed with an unbalanced Mach-Zehnder interferometry setup, as in ref. [28], in parallel and orthogonal polarization configurations. The outputs of this interferometer are detected by single-mode fiber-coupled single-photon counters. For both XX and X photon, a record of coincidence events is kept to build up a time-delayed histogram as shown in Fig. 4. In both cases, we observe a strong suppression of the coincidences at zero delay when the two photons are in the parallel polarization.

Raw interference visibilities extracted from the areas of the central peaks for the XX and X photons are 0.86(1) and 0.67(1), respectively. Taking into account of the residual two-photon events probability and the independently calibrated optical imperfections of our interferometric set-up, a corrected degree of indistinguishability for the XX and X photons are estimated to be 0.90(1) and 0.71(1), respectively. A closer inspection of the coincidence counts in Fig. 4b-d shows a dip around the zero delay due to temporal filtering by ultrafast timing resolution (~20 ps) of the superconducting nanowire single-photon detectors, which improves the interference visibility to 0.93(2) and 0.86(3) for the XX and X photons, respectively. Note the XX photon shows a significantly better indistinguishability than the X photon. This could be due to the fact that the X photon

inherits an emission time uncertainty from the lifetime of the XX photon which is 66.4 ps. Thus, in applications such as entanglement swapping [37], it would be advantageous to choose the XX photons for interference to obtain a high visibility.

In summary, by pulsed two-photon resonant excitation of a quantum dot embedded in a CBG bullseye cavity, we have realized a deterministic entangled photon pair source with simultaneously an entanglement fidelity of 90%, a photon extraction efficiency of 79%, and photon indistinguishability up to 93%. Using actively de-multiplexing with electro-optical modulators as demonstrated in multi-photon boson sampling [38], the single entangled-photon pair source realized here can be readily extended to multiple entanglement source. Immediately applications [25-27] include heralded multi-photon entanglement, entanglement swapping and purification, and boson sampling, which can be performed without the complication of higher-order emissions, a notorious problem in parametric down-conversion [10].

Future work is planned to apply surface passivation during the CBG fabrication to reduce the blinking and spectral diffusion. To improve the device yield, it is desirable to combine deterministic emitter positioning for an optimal spatial coupling and in-situ strain tuning for minimize the fine structure splitting for the engineering of solid-state sources of photon pairs with near-unity degrees of entanglement, indistinguishability, and efficiency.

References:

[1] E. Schrodinger, The Present Situation in Quantum Mechanics. *Proceedings of the American Philosophical Society* (Nov. 29, 1935).

[2] C. S. Wu, I. Shaknov, *Phys. Rev.* **77**, 136 (1950).

[3] J. S. Bell, *Physics* **1,** 195 (1964).

[4] A. Einstein, B. Podolsky, N. Rosen, *Phys. Rev.* **47**, 777 (1935).

[5] A. K. Ekert, *Phys. Rev. Lett.* **67**, 661 (1991).

[6] C. H. Bennett, *et al.*, *Phys. Rev. Lett.* **70**, 1895 (1993).

[7] V. Giovannetti, S. Lloyd, L. Maccone, *Phys. Rev. Lett.* **96**, 010401 (2006).

[8] R. Raussendorf, H. J. Briegel, *Phys. Rev. Lett.* **86**, 5188 (2001).

[9] S. J. Freedman, J. F. Clauser, *Phys. Rev. Lett.* **28**, 938 (1972).

[10] P. G. Kwiat, K. Mattle, H. Weinfurter, A. Zeilinger, A. V. Sergienko, Y. Shih, *Phys. Rev. Lett.* **75**, 4337 (1995).

[11] O. Benson, C. Santori, M. Pelton, Y. Yamamoto, *Phys. Rev. Lett.* **84**, 2513 (2000).

[12] C.-Y. Lu, J.-W. Pan, *Nature Photonics* **8**, 174 (2014).

[13] M. Giustina *et al.*, *Phys. Rev. Lett.* **115**, 250401 (2015).

[14] L. K. Shalm *et al.*, *Phys. Rev. Lett.* **115**, 250402 (2015).

[15] H.-S. Zhong *et al.*, *Phys. Rev. Lett.*, to appear (2018).

[16] N. Akopian *et al.*, *Phys. Rev. Lett.* **96**, 130501 (2006). R. J. Young, *et al.*, *New J. Phys.* **8**, 29 (2006). A. Muller, W. Fang, J. Lawall, G S. Solomon, *Phys. Rev. Lett.* **103**, 217402 (2009). T. H. Chung *et al.*, *Nat. Photon.* **10**, 782 (2016).

[17] Y. H. Huo, A. Rastelli, O. G. Schmidt, *Appl. Phys. Lett.* **102**,152105 (2013). T. Kuroda, *et al. Phys. Rev. B* **88**, 041306 (2013).

[18] D. Huber *et al.*, *Phys. Rev. Lett.* **121**, 033902 (2018).

[19] A. Dousse *et al.*, *Nature* **466**, 217 (2010).

[20] M. A. M. Versteegh, *et al. Nature Communications* **5**, 5298 (2014).

[21] K. D. Jöns, *et al. Sci. Rep.* **7**, 1700 (2017).

[22] Y. Chen, M. Zopf, R. Keil, F. Ding, O. G. Schmidt, *Nature Communications* **9**, 2994 (2018).

[23] M. Muller, S. Bounouar, K. D. Jons, M. Glass, P. Michler, *Nat. Photon.* **8**, 224 (2014).

[24] R. M. Stevenson, C. L. Salter, J. Nilsson, A. J. Bennett, M. B. Ward, I. Farrer, D. A. Ritchie, A. J. Shields, *Phys. Rev. Lett.* **108**, 040503 (2012). D. Huber, M. Reindl, Y. H. Huo, H. Y. Huang, J. S. Wildmann, O. G. Schmidt, A. Rastelli, R. Trotta, *Nat. Commun.* **10**, 15506 (2017).

[25] H.-J. Briegel, W. Dur, J. I. Cirac, P. Zoller, *Phys. Rev. Lett.* **81**, 5932 (1998).

[26] P. Kok, W. J. Munro, K. Nemoto, T. C. Ralph, J. P. Dowling, G. J. Milburn, *Rev. Mod. Phys.* **79**, 135 (2007). J.-W. Pan, Z.-Bing Chen, C.-Y. Lu, H. Weinfurter, A. Zeilinger, M. Żukowski, *Rev. Mod. Phys.* **84**, 777 (2012).

[27] D. E. Browne, T. Rudolph, *Phys. Rev. Lett.* **95**, 010501 (2005). T. Rudolph, *APL Photonics* **2**, 030901 (2017).

[28] X. Ding, *et al. Phys. Rev. Lett.* **116**, 020401 (2016). N. Somaschi *et al.*, *Nat. Photonics* **10**, 340 (2016). Y.-M. He, arXiv. 1809.10992 (2018).

[29] A. J. Shields, *Nature Photonics* **1**, 215 (2007); S. Buckley, K. Rivoire, J. Vuĉković, *Rep. Prog. Phys.* **75**, 126503 (2012). P. Lodahl, S. Mahmoodian, S. Stobbe, *Rev. Mod. Phys.* **87**, 347 (2015). A. Orieux, M. A. M Versteegh, K. D. Jons S. Ducci, *Rep. Prog. Phys.* **80**, 076001(2017).

[30] A. V. Kuhlmann, *et al. Nat. Commun.* **6**, 8204 (2015). H. Wang *et al. Phys. Rev. Lett.* **116**, 213601 (2016).

[31] W. M. J. Green, J. Scheuer, G. DeRose, A. Yariv, *Appl. Phys. Lett.* **85**, 3669 (2004). M. Y. Su, R. P. Mirin, *Appl. Phys. Lett.* **89**, 033105 (2006).

[32] M. Davanco, M. T. Rakher, D. Schuh, A. Badolato, K. Srinivasan, *Appl. Phys. Lett.* **99**, 041102 (2011). L. Sapienza, M. Davano, A. Badolato, K. Srinivasan, *Nat. Commun.* **6**, 7833 (2015).

[33] L. Li *et al. Nano Lett.* **15**, 1493 (2015).

[34] M. E. Reimer, *et al. Nat. Commun.* **3**, 737 (2012).

[35] X.-W. Chen, S. Gotzinger, V. Sandoghdar, *Opt. Lett.* **36**, 3545 (2011). A. W. Schell, *et al. App. Phys. Lett.* **105**, 231117 (2014). Y. Ma, P. E. Kremer, B. D. Gerardot, *J. App. Phys.* **115**, 023106 (2014). S. Fischbach *et al. App. Phys. Lett.* **111**, 011106 (2017). B. Yao, R. Su, Y. Wei, Z. Liu, T. Zhao, J. Liu, *J. Kore. Phys. Soc.* **73**, 1502 (2018)

[36] L. Schweickert, *et al. App. Phys. Lett.* **112**, 093106 (2018)

[37] M. Zukowski, A. Zeilinger, M. A. Horne, A. K. Ekert, *Phys. Rev. Lett.* **71**, 4287 (1993).

[38] H. Wang, *et al. Nature Photonics* **11**, 361 (2017).

Figure captions:

Figure 1: **Nanostructure and simulation of circular Bragg grating (CBG) cavity in a bullseye geometry**. (**a**) Top view of a scanning electron microscope image of the CBG cavity in X-Y plane. (**b**) Side view of our device. The design parameters of the CBG are labelled. (**c**) Numerical simulation of the single-photon extraction efficiency and Purcell factor as a function of photon emission wavelength indicates a broadband feature of the CBG cavity. (**d**) Numerical simulation of far-field distribution of the electrical field intensity of the emission assuming an emitter sitting in the center of the CBG.

Figure 2: **Brightness and purity of the XX and X photons**. (**a**) The spectrum of the cascaded emitted XX and X photons from the level structure shown in the inset. The energy of the pulsed laser for excitation is set at the average energy of the XX and X photons, in resonance with the virtual biexciton two-photon excitation state. (**b**) The eventually detected single photon counts as a function of the square root of excitation laser power, showing a clear Rabi oscillation. (**c**) Measurement of time-resolved XX and X photon counts to determine their lifetime. (**d**) Intensity-correlation histogram of the XX and X photons under π pulse excitation, obtained using a Hanbury Brown and Twiss-type setup.

Figure 3: **Measurement of two-photon entanglement fidelity**. (**a**) Detected XX-X cross-correlation coincidence counts in linear basis. H: horizontal. V: vertical. (**b**) in diagonal basis. D: +45°. A: -45°. (**c**) in circular basis. R: right circular. L: left circular. The graphs for co-polarized (red) and cross-polarized (blue) photons are temporally shifted by 2 ns for clarity.

Figure 4: **Indistinguishability of the XX and X photons**. The interference between two XX photons is plotted in (**a**) and (**b**). The same data for X photons is shown in (**c**) and (**d**). The input two photons are π-pulse excited and prepared in cross (**a**), (**c**) and parallel (**b**), (**d**) polarizations, respectively. The fitting function is the convolution of exponential decay (emitter decay response) with Gaussian (photon detection time response). All the data points presented are raw data without background subtraction.

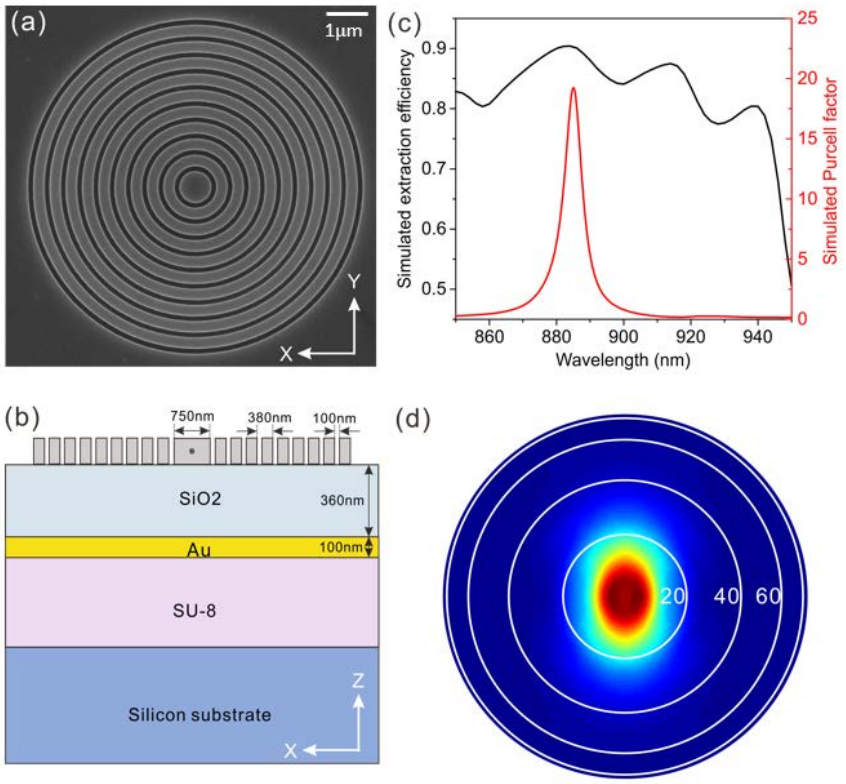

Figure 1

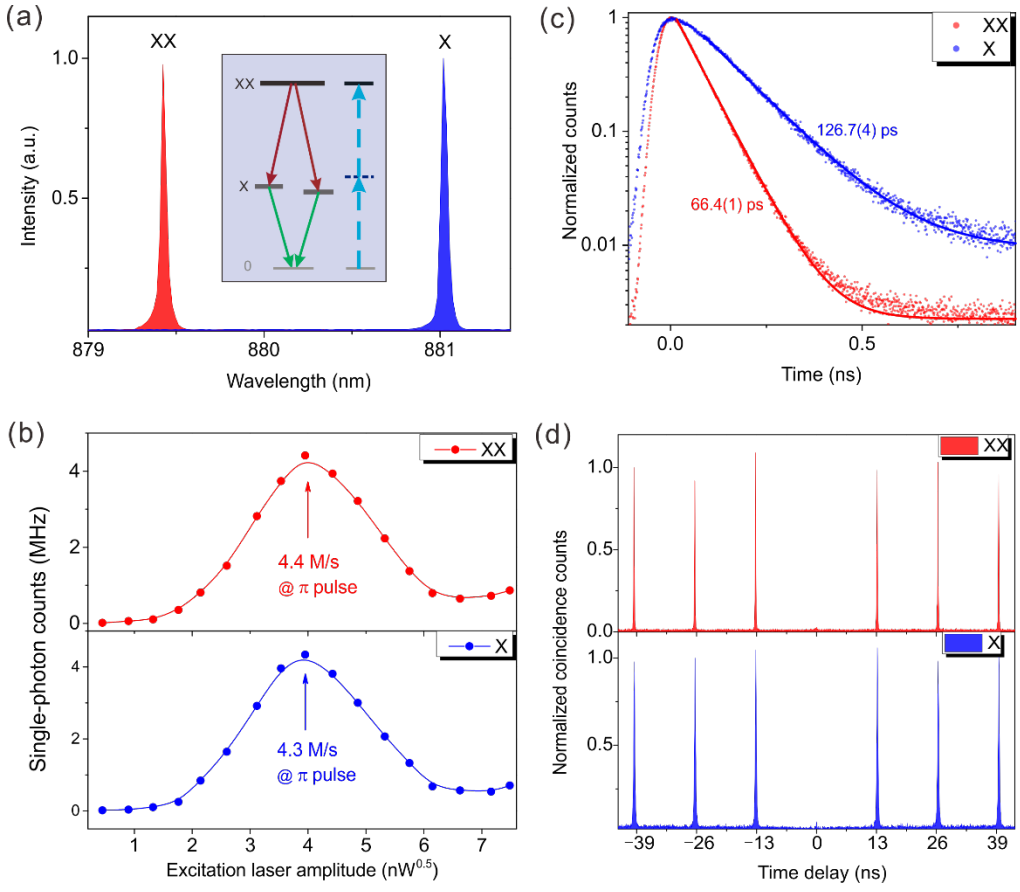

Figure 2

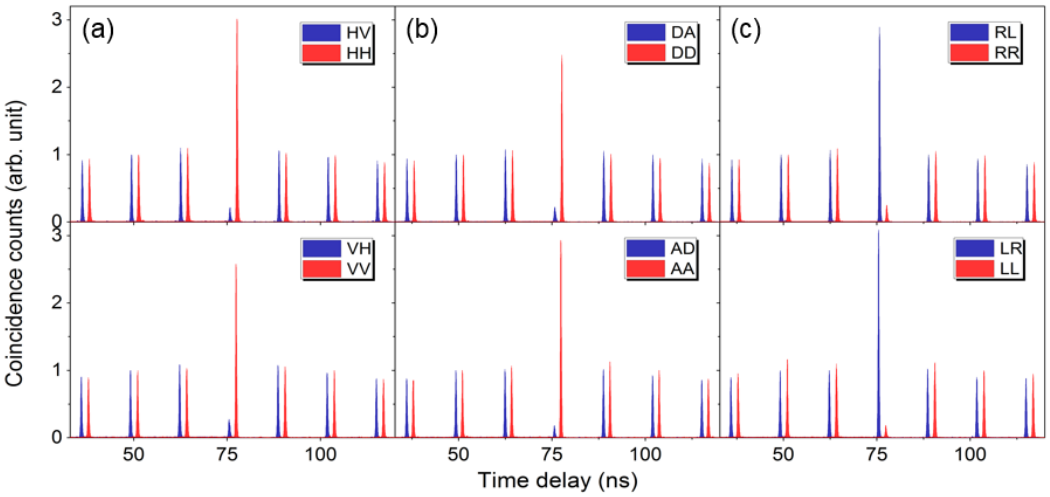

Figure 3

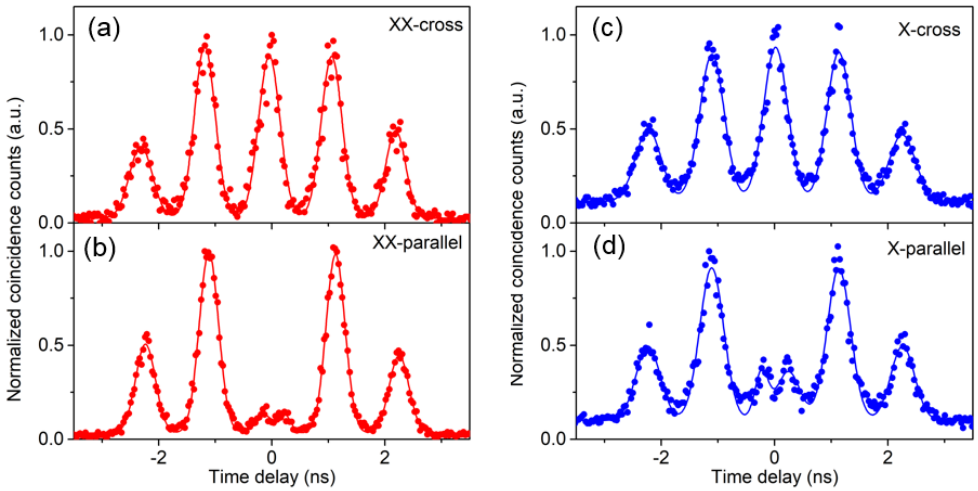

Figure 4